Available online at www.sciencedirect.com
SCIENCE DIRECT®
ELSEVIER
Journal of Sound and Vibration 287 (2005) 1013–1026
JOURNAL OF SOUND AND VIBRATION
www.elsevier.com/locate/jsvi

Short Communication

Free vibration of composite re-bars in reinforced structures

Fethi Kadioglu*

Faculty of Civil Engineering, Istanbul Technical University, ITU, 34469 Maslak, Istanbul, Turkey

Received 3 March 2004; received in revised form 17 February 2005; accepted 23 February 2005
Available online 13 May 2005

Abstract

The effect of composite rebar's shape in reinforced concrete beam-type structures on the natural frequencies and modes shapes is investigated through finite element analysis in this paper. Steel rebars are being replaced with composite rebars due to their better ability to resist corrosion in reinforced concrete structures for many infrastructure applications. A variety of composite rebar shapes can be obtained through the pultrusion process. It will be interesting to investigate their shape on free vibration characteristics. The results of natural frequencies and mode shapes are presented and compared for the different composite rebar shapes. The effects of various boundary conditions for different rebar shapes are also investigated.

1. Introduction

Composite rebar technology has received considerable attention in recent years [1–6] as it offers significant advantages over steel reinforced concrete structures, including improved static and dynamic behavior. Dynamic analysis of composite structures is of practical importance in many engineering applications, especially where vibratory loads are applied. Composite rebars made from either glass fiber-reinforced polymer or aramid fiber-reinforced polymer or carbon fiber-reinforced can be readily formed into complex shapes through the pultrusion manufacturing process. In the pultrusion process, the longitudinal fibers are drawn through a resin bath and then passed through a die, which gives the rebar a final shape. In general, a smooth surface is obtained

*Tel.: +90 212 285 3706; fax: +90 212 285 6587.
E-mail address: fkadioglu@itu.edu.tr.

0022-460X/$ - see front matter
doi:10.1016/j.jsv.2005.02.039

on the rebars through pultrusion process, and additional techniques are required to improve the bond between the rebar and the surrounding concrete. Several methods [7–9] have been developed to improve the bond characteristic of the composite rebars. These include double wrapping of a helical fiber around the rebar, machining of rebars, embedding sand particles, sand blasting, etc. All of the above techniques involve introducing deformations on the surface of rebar to improve the bond.

Lee and Kim [10,11] investigated free vibration of thin-walled laminated composite beams. Their equations of motion are derived from the Hamilton's principle. They also demonstrated the coupling of flexural and torsional modes for arbitrary laminate stacking sequence configuration. Matsuga [12] studied natural frequencies and buckling stresses of laminated composite beams by taking into account the complete effect of transverse shear and normal stresses and rotatory inertia. Several authors [13–17] studied the free vibrations of composite rebars both analyticaly and numerically. Pidaparti and Liu [18] presented three-dimensional linear finite element computations to investigate the free vibration response of two-ply cord-rubber composite structures. Banerjee and Williams [19] discussed an exact dynamic stiffness matrix for a composite Timoshenko beam. It includes the effects of shear deformation and rotatory inertia. Marur and Kant [20] proposed three higher order refined displacement models for the free vibration analysis of sandwich and composite beams. Recently, Kadioglu and Pidaparti [21] presented the effectiveness of composite rebar configurations in beam-type reinforced concrete structures under different static loadings.

Based on the literature review, it appears that the effect of composite rebar configura tions in reinforced structures on the natural frequencies and modes shapes has not yet been investigated. The objective of this study is to investigate the free vibration characteristics of various composite rebar configurations embedded in concrete beam. Specifically, four different composite rebar configurations under free vibration with different boundary conditions are investigated using three-dimensional finite element analysis. The results of natural frequencies and modes shapes obtained are presented to illustrate the effectiveness of composite rebar configurations for dynamic applications in beam-type reinforced concrete structures.

2. Composite rebar configurations

Four different types of composite rebar configurations of different means for improving the bond properties shown in Fig. 1 are considered with the surrounding concrete. The first rebar (RB1) is a standard circular cross-section that is commonly used in construction industry. The second rebar (RB2) has a circular cross-section, but with helical wrapping/deformation on the surface. The composite rebar RB3 is of square cross-section, and the rebar RB4 is a circular rebar with square sections at midsides. The idea of using ribs is to improve the bond characteristics with the surrounding concrete. There might be several other possible variations of these rebar configurations, but they are beyond the scope of this study. All the rebars are made from either fiber-reinforced polymer composites or steel. These various composite rebars configurations can be easily manufactured through the pultrusion process.

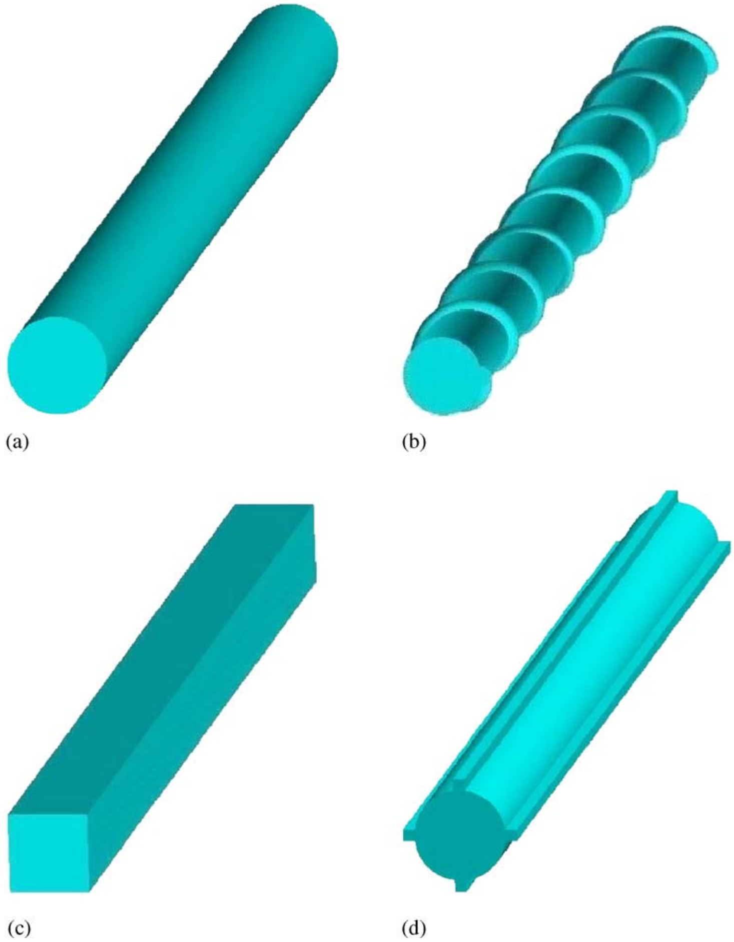

Fig. 1. Various rebars considered for use in reinforced structures: (a) RB1—circular rebar; (b) RB2—circular rebar with helical wrap; (c) RB3—square rebar; (d) RB4—circular rebar with four ribs.

3. Finite element analysis

Free vibration analyses of various rebar configurations embedded in concrete are investigated through a three-dimensional finite element analysis. The composite rebar having a configuration (circular, square, circular with ribs, etc.) and enclosed in concrete block is considered for analysis. The composite rebar and the surrounding concrete are modeled using three-dimensional finite elements in ANSYS software [22]. It is assumed that the interface between the rebar and the surrounding concrete is perfect. This assumption may not be true and, should be evaluated in the future for realistic analysis. Both the composite rebar and the concrete are modeled using a 3D isoparametric brick element designated as SOLID45 in ANSYS software. The SOLID45 element type is defined by eight nodes and has three degrees of freedom (translations in x, y, and z directions) at each node. For rebar with helical warping, beam elements (BEAM 4 in ANSYS

Software) were used to model the helical warping. Free mesh is used for creating the finite element model. The boundary conditions for the finite element model are assumed to be at one end fixed, and at the other free, unless otherwise specified.

A typical unit consisting of composite rebars 3 m long embedded in a concrete block of dimensions ($D/d = 2$; and $L/d = 24$) are considered for free vibration analysis. For all the cases, it is assumed that the composite rebar shape is different, but the concrete is the same surrounding the rebar. The geometry and boundary conditions are shown in Fig. 2. Linear material models are assumed for both the concrete and the composite rebar. The natural frequencies, and mode shapes are obtained from the free vibration analysis.

The materials properties for the concrete used in the finite element analysis are Young's modulus, $E = 30\,\text{GPa}$, density, $\rho = 2400\,\text{kg/m}^3$ and Poisson's ratio, $\nu = 0.15$. Three different elastic properties were used for the composite rebar. The materials properties for the composite rebar are Glass-Epoxy ($E_1 = 54\,\text{GPa}$; $E_2 = E_3 = 18\,\text{GPa}$; $G_{12} = 9\,\text{GPa}$, $\nu_{12} = 0.25$), Carbon-Epoxy ($E_1 = 132\,\text{GPa}$; $E_2 = E_3 = 11.2\,\text{GPa}$; $G_{12} = 6.55\,\text{GPa}$, $\nu_{12} = 0.28$) and Graphite-Epoxy ($E_1 = 210\,\text{GPa}$; $E_2 = E_3 = 5\,\text{GPa}$; $G_{12} = 2.6\,\text{GPa}$, $\nu_{12} = 0.25$) using density, $\rho = 1400\,\text{kg/m}^3$. The finite element meshes for obtaining the stresses are based on a convergence study with an accuracy of 1% between consecutive meshes. The results are obtained using the finite element meshes of 8620, 7024, 8580 and 9060, for RB1, RB2, RB3 and RB4, respectively. The results of natural frequencies are obtained for all the cases and presented to illustrate the differences due to various rebar configurations.

4. Results and discussion

The results of natural frequencies and mode shapes are presented for the different composite rebar shapes. The frequency values are calculated for all examples under fixed-free boundary condition using a rebar elastic modulus of 210 GPa, and graphite-epoxy, for isotropic and orthotropic rebars embedded in concrete, respectively.

4.1. Validation

The finite element results of natural frequencies and mode shapes for circular rebar RB1 under free vibration without concrete are obtained from finite element analysis. The present finite element model was validated by comparing the results of the natural frequencies obtained to the analytical solution using beam theory [23], as no other results are available for comparison in the literature. In Table 1 is shown the comparison of the first three bending and torsion modes in the $x-y$ plane and first two axial modes. It can be seen from Table 1 that there is a 0.5% difference in the results between the beam theory and three-dimensional finite element analysis. The results presented in Table 1 demonstrate the validity of the present finite element model for three-dimensional free vibration analysis of composite rebar structures.

In Fig. 3 are shown the first three vibration mode shapes for bending, torsion frequencies, and two axial vibration modes. Table 2 shows the comparison of bending frequencies values (Hz) under fix-free boundary condition for various rebar configurations considered in Fig. 1 with the surrounding concrete. The frequency values are calculated for both isotropic and orthotropic

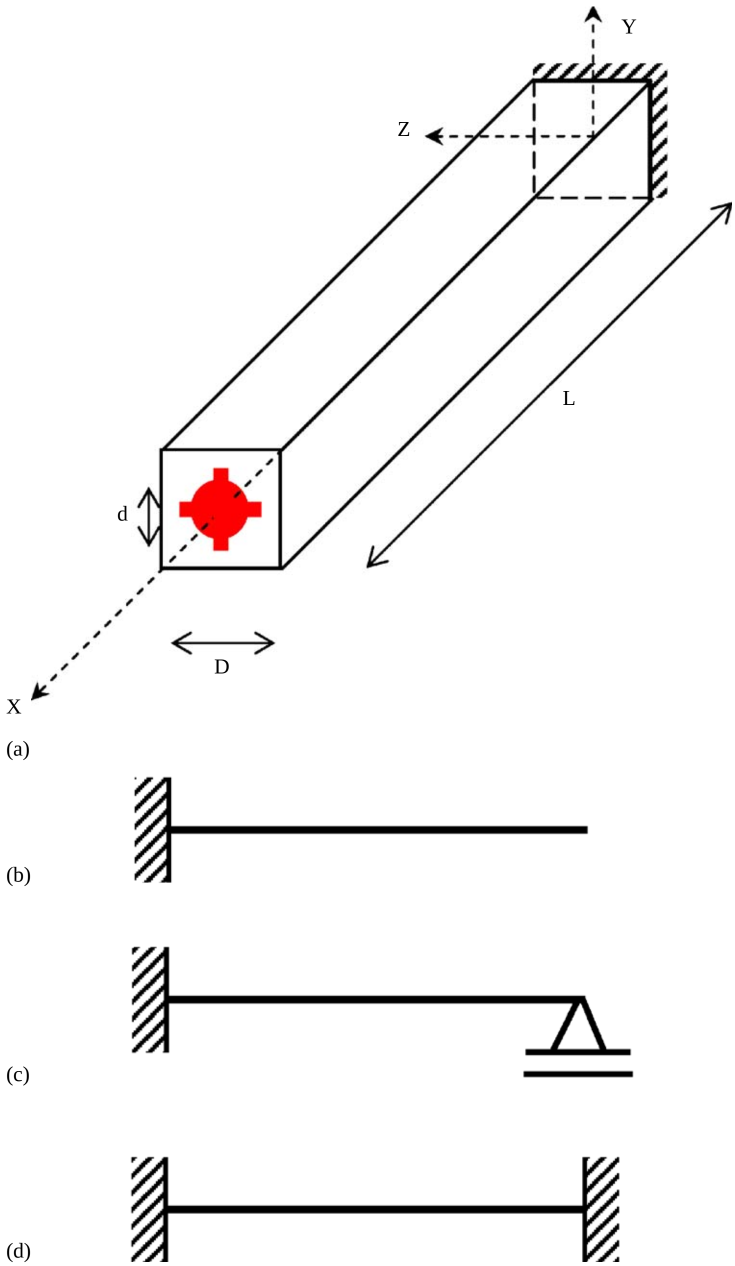

Fig. 2. Geometry of a typical unit of rebar with concrete along with boundary conditions considered for finite element analysis: (a) Geometry of a typical reinforced concrete structure; (b–d) boundary conditions for case-1, case-2 and case-3, respectively.

using a rebar modulus (E) of 210 GPa. It can be seen from Table 2 that all the frequency values decrease for RB1, RB2 and RB4 as compared to RB3, the square rebar. It is also seen that the frequency decrease for RB2 is smaller as compared to the increase for rebars RB3 and RB4. All

Table 1
A comparison of bending natural frequency values (Hz) for isotropic rebars with analytical solution under fix-free boundary condition

Vibration modes	RB1	Analytical solution [23]
Bending		
Mode-1	23.95	23.79
Mode-2	150.11	149.13
Mode-3	421.393	417.58
Axial		
Mode-1	1023	1021
Mode-2	3077	3062
Torsion		
Mode-1	645.56	645.5
Mode-2	1940.7	1936.5
Mode-3	3247.7	3227.5

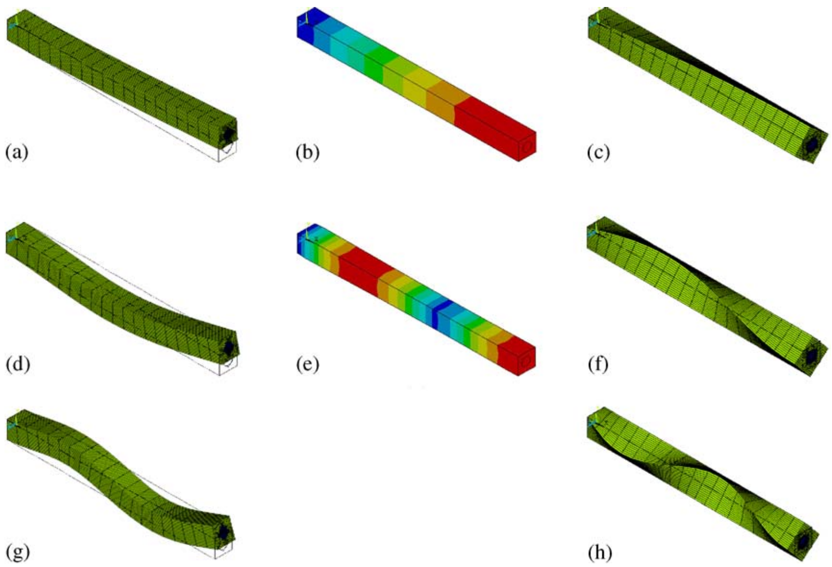

Fig. 3. Bending, axial and torsional mode shapes for isotropic rebar vibration under Fix-Free boundary condition: (a) bending, mode-1; (b) axial, mode-1; (c) torsion, mode-1; (d) bending, mode-2; (e) axial, mode-2; (f) torsion, mode-2; (g) bending, mode-3; (h) torsion, mode-3.

the frequency values for isotropic and orthotropic are within 10% for RB3 as compared to RB1. The first, second and third frequency values increase about 8% for RB3 in comparison to RB1. The large increase in frequency for rebar RB3 is due to increase in the stiffness of the rebar as compared to other rebars configurations. In Table 3 is shown the results of the first two axial modes. The results of the first three torsion modes presented in Table 4. It can be seen from

Table 2
Comparison of bending frequency values (Hz) for fix-free boundary condition

	RB1	RB2	RB3	RB4
(a) *First bending frequency values*				
Mode-1				
Isotropic	18.285	18.261	19.662	18.687
Orthotropic	18.128	18.071	19.442	18.512
(b) *Second bending frequency values*				
Mode-2				
Isotropic	112.794	112.6	121.371	115.301
Orthotropic	108.211	107.875	114.466	110.013
(c) *Third bending frequency values*				
Mode-3				
Isotropic	309.085	308.517	332.888	316.056
Orthotropic	284.395	283.435	296.231	287.664

Table 3
Comparison of axial frequency values (Hz) for fix-free boundary condition

	RB1	RB2	RB3	RB4
(a) *First axial frequency values*				
Mode-1				
Isotropic	454.016	452.732	493.332	465.553
Orthotropic	452.156	450.56	490.964	463.571
(b) *Second axial frequency value*				
Mode-2				
Isotropic	1358	1342	1475	1392
Orthotropic	1331	1329	1440	1364

Table 4 that there is a maximum 16% difference in the results between the isotropic and orthotropic rebars for RB3.

4.2. *Effect of boundary conditions*

Table 5 shows the comparison of bending frequency values (Hz) under different boundary condition for various orthotropic rebar configurations considered in Fig. 1. The frequency values are calculated for orthotropic rebar using the properties of graphite-epoxy. It can be seen that the fixed-free boundary condition has the lowest frequencies, as compared to the other boundary conditions considered. Fixed-fixed boundary condition has the largest natural frequencies. The vibration frequencies strongly depend on the boundary conditions. Based on the summary of results presented in Table 5 indicates that a circular rebar with 4 ribs, RB3, has maximum higher

Table 4
Comparison of torsion frequency values (Hz) for fix-free boundary condition

	RB1	RB2	RB3	RB4
(a) *First torsion frequency values*				
Mode-1				
Isotropic	200.370	200.297	210.616	202.571
Orthotropic	177.26	177.16	175.791	176.003
(b) *Second torsion frequency values*				
Mode-2				
Isotropic	602.026	601.783	632.737	608.631
Orthotropic	532.874	532.552	528.457	529.109
(c) *Third torsion frequency values*				
Mode-3				
Isotropic	1006.3	1005.9	1058	1017
Orthotropic	891.783	891.597	884.378	885.524

Table 5
Comparison of bending frequency values (Hz) for orthotropic rebars with different boundary conditions

B.C.	RB1	RB2	RB3	RB4
Mode-1				
Case-1	18.128	18.071	19.442	18.512
Case-2	76.538	76.296	81.092	77.853
Case-3	107.910	107.564	113.317	109.436
Mode-2				
Case-1	108.211	107.875	114.466	110.013
Case-2	232.070	231.302	241.673	234.719
Case-3	275.983	275.058	284.741	278.263
Mode-3				
Case-1	284.395	283.435	296.231	287.664
Case-2	448.085	446.511	459.116	450.733
Case-3	501.292	499.498	510.025	503.046

bending frequency. It is also seen from Table 5 that the increase in bending frequency is about 489% and 133% when the frequency is increased from first to second and from second to third mode shapes for fixed-free boundary condition. Similarly, the increase in bending frequency is about 317% and 483% for RB3 when boundary conditions are changed from fixed-free to fixed-hinged and fixed-fixed.

4.3. *Effect of design features*

In order to see how other design features affect the frequency values, RB4 is investigated further. The design features evaluated include number of ribs, and also the orientation of the ribs

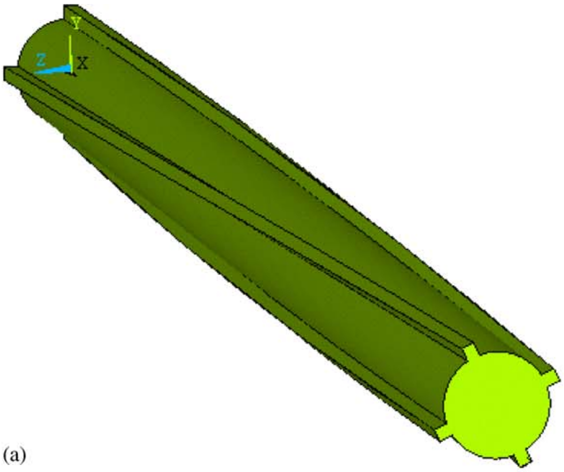

(a)

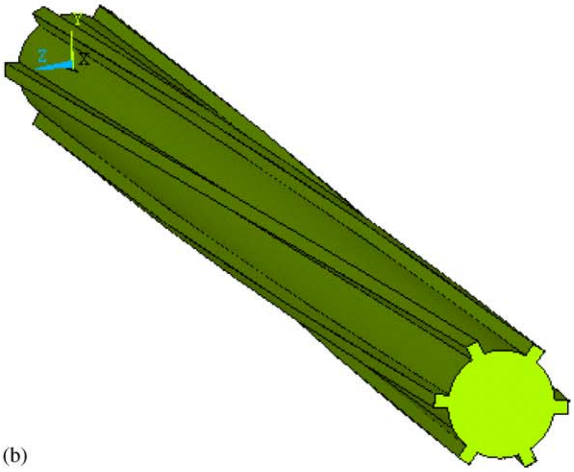

(b)

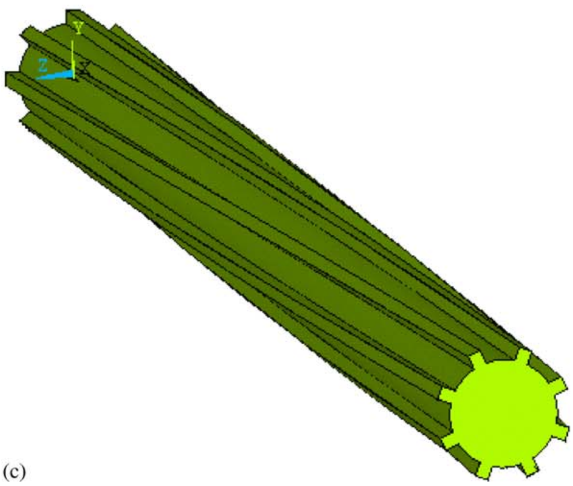

(c)

Fig. 4. Design features (number of ribs and off-set) considered for rebar RB4: (a) circular rebar with 4 square ribs and 2° off-set; (b) circular rebar with 6 square ribs and 2° off-set; (c) circular rebar with 8 square ribs and 2° off-set.

Table 6
A comparison of natural frequency values (Hz) for orthotropic 2° off-set rebar under fix-free boundary condition

Modes	4 ribs	6 ribs	8 ribs
Bending			
Mode-1	19.076	19.268	19.482
Mode-2	112.984	113.959	115.053
Mode-3	293.941	296.036	298.506
Axial			
Mode-1	463.555	469.295	474.733
Mode-2	1363.4	1380.2	1396.2
Torsion			
Mode-1	182.443	182.015	181.608
Mode-2	549.135	547.082	545.221
Mode-3	916.257	913.815	910.753

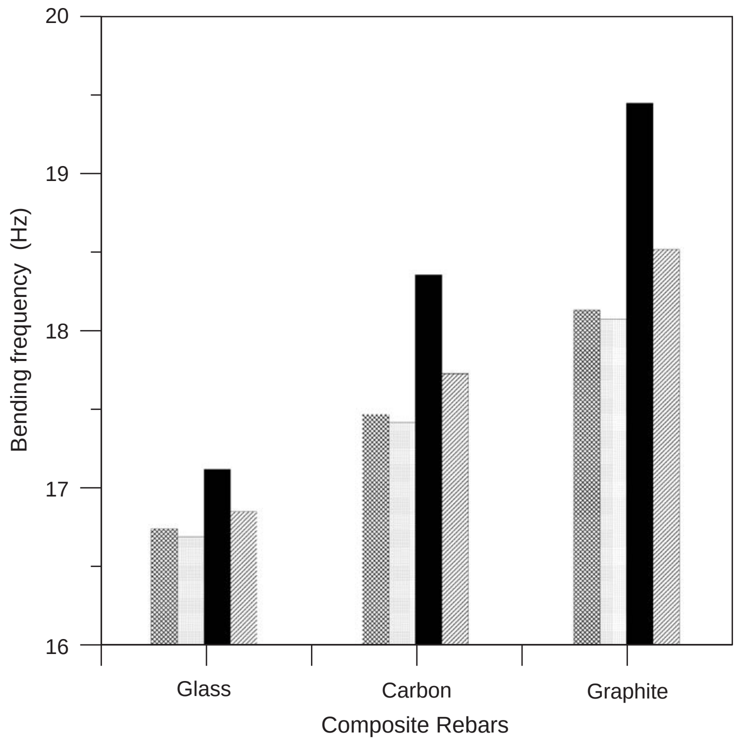

Fig. 5. Variation of bending natural frequency (Hz) for orthotropic rebars with various composite materials under fix-free boundary condition. RB1: ▩; RB2: ▤; RB3: ■; RB4: ▨.

at an offset angle. The typical geometry of the circular rebar with 4, 6 and 8 ribs with a 2 offset orientation is shown in Fig. 4. A typical finite element mesh for the offset rebars was modeled using SOLID92 (10-node tetrahedral) and SOLID45 (8-node structural) elements due to geometry of the rebars embedded in concrete beam. The meshes for these offset rebars range from 11296 to 13343 elements in order to get good results for frequency. The results of frequency values obtained for offset rebars are compared to circular rebar RB1. The properties of graphite-epoxy were used for the rebars in this example under fixed-free boundary condition. The results are summarized in Table 6. It can be seen from Table 6 that there is increase about 2% in bending and axial frequency, but decrease about 0.5% in torsion frequency from 4 ribs to 8 ribs.

4.4. Effect of composite properties

In order to see how the composite properties change the natural frequency various values of Glass/Carbon and Graphite-epoxy considered. The results of first bending, axial and torsional frequency values for fix-free boundary condition with RB1, RB2, RB3 and RB4 combinations embedded in concrete beam under free vibration are summarized in Figs. 5–7. The frequencies are calculated based on the properties of concrete ($E = 30\,\text{GPa}$). It can be seen from Fig. 5 that increasing elastic modulus (E) increases frequency values for orthotropic rebar. It is also seen from Fig. 5 that the increase in frequency values is about 5% and 11% when the elastic modulus are increased from glass-epoxy to carbon-epoxy and graphite-epoxy keeping the concrete properties the same at fix-free boundary condition. Similar trends to those shown in Fig. 5 are also observed for the four rebars configurations in axial frequency (see Fig. 6). Overall, the results

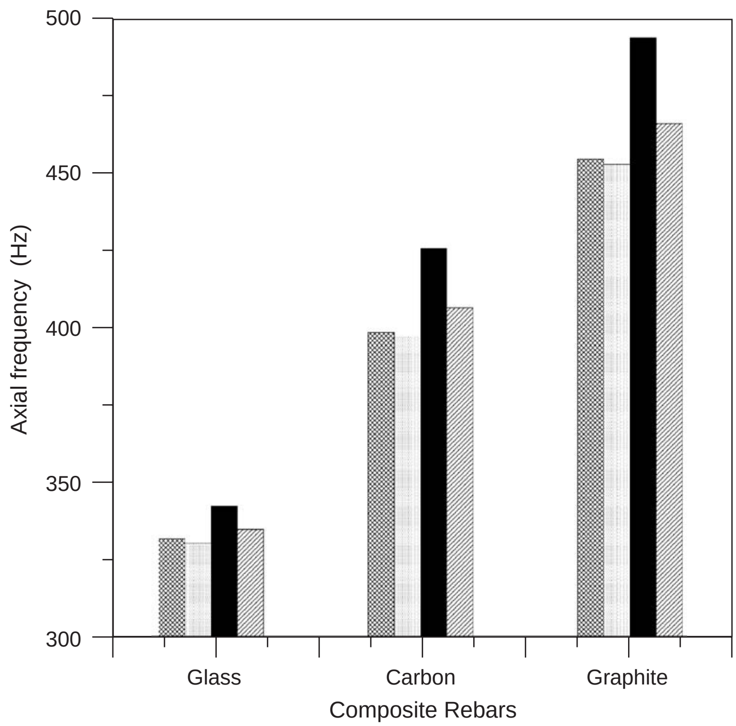

Fig. 6. Variation of axial natural frequency (Hz) for orthotropic rebars with various composite materials under fix-free boundary condition. RB1: ▩; RB2: ▤; RB3: ■; RB4: ▨.

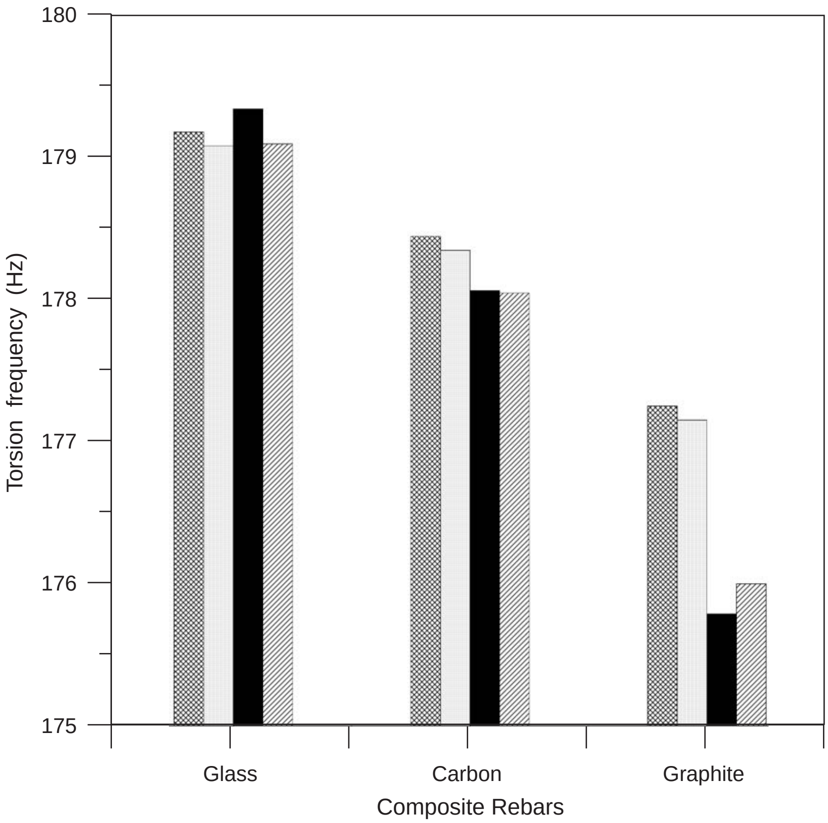

Fig. 7. Variation of torsion natural frequency (Hz) for orthotropic rebars with various composite materials under fix-free boundary condition. RB1: ▩; RB2: ▤; RB3: ■; RB4:▨.

presented in Fig. 6 along with others may provide some insight on the effect of design features on rebar frequency for free vibration. It can be seen from Fig. 7 that there is a decrease of about 1% in torsion frequency values for composite rebars, when the rebar material is changed from glass-epoxy to carbon-epoxy and graphite-epoxy. Overall the results presented in Figs. 5–7 represent how the rebar properties affect the frequency for free vibration.

5. Conclusions

Free vibration analyses of various composite rebar configurations for use in concrete structures is investigated through a three-dimensional finite element method. The composite rebar configurations investigated include square rebar, circular rebar with ribs, and ribs oriented at an offset angle along the length of the rebar. Results of natural frequencies obtained are presented and compared among various rebar configurations. Many more cases need to be studied in order to find optimum rebar configuration for use. The results presented in this paper illustrate that various design features added to the circular composite rebar may provide good vibration characteristics and can be used in reinforced concrete structures.

Acknowledgements

The author acknowledges the support from the Scientific and Technical Research Council of Turkey under a grant in the scope of NATO Science Fellowship Program. The author thanks Professor Dr. Ramana PIDAPARTI for his help during the course of this study. The author thanks the NSF for supporting this work through a Grant INT-0096795.

References

[1] S.N. Luo, F. Yi-Ming, C. Zhi-Yuan, Non-linear vibration of composite beams with an arbitrary delamination, *Journal of Sound and Vibration* 271 (2004) 535–545.
[2] H. Arya, A new zig-zag model for laminated composite beams: free vibration analysis, *Journal of Sound and Vibration* 264 (2003) 485–490.
[3] J.R. Banerjee, Free vibration of sandwich beams using the dynamic stiffness method, *Computers and Structures* 81 (2003) 1915–1922.
[4] H. Waisman, H. Abramovich, Variation of natural frequencies of beams using the active stiffening effect, *Composites: Part B* 33 (2002) 415–424.
[5] A. Zak, M. Krawczuk, W. Ostachowicz, Numerical and experimental investigation of free vibration of multilayer delaminated composite beams and plates, *Computational Mechanics* 26 (2000) 309–315.
[6] J. Lee, Free vibration analysis of delaminated composite beams, *Computers and Structures* 74 (2000) 121–129.
[7] H. Nordin, B. Taljsten, Testing of hybrid FRP composite beams in bending, *Composites: Part B* 35 (2004) 27–33.
[8] G.S. Ramtekkar, Y.M. Desai, Natural vibrations of laminated composite beams by using mixed finite element modeling, *Journal of Sound and Vibration* 257 (2002) 635–651.
[9] M.K. Rao, Y.M. Desai, M.R. Chitnis, Free vibrations of laminated beams using mixed theory, *Composite Structures* 52 (2001) 149–160.
[10] J. Lee, S.E. Kim, Free vibration of thin-walled composite beams with I-shaped cross-sections, *Composite Structures* 55 (2002) 205–215.
[11] J. Lee, S.E. Kim, Flexural-torsional coupled vibration of thin-walled composite beams with channel sections, *Computers and Structures* 80 (2002) 133–144.
[12] H. Matsunaga, Vibration and buckling of multilayered composite beams according to higher order deformation theories, *Journal of Sound and Vibration* 246 (2001) 47–62.
[13] J.R. Banerjee, Frequency equation and mode shape formulae for composite Timoshenko beams, *Composite Structures* 51 (2001) 381–388.
[14] G. Shi, K.Y. Lam, Finite element vibration analysis of composite beams based on higher-order beam theory, *Journal of Sound and Vibration* 219 (1999) 707–721.
[15] J.R. Banerjee, Free vibration of axially loaded composite Timoshenko beams using the dynamic stiffness matrix method, *Computers and Structures* 69 (1998) 197–208.
[16] R. Suresh, S.K. Malhotra, Vibration and damping analysis of thin-walled box beams, *Journal of Sound and Vibration* 215 (1998) 201–210.
[17] S.R. Rao, N. Ganesan, Dynamic response of non-uniform composite beams, *Journal of Sound and Vibration* 200 (1997) 563–577.
[18] R.M. Pidaparti, Y. Liu, Free vibration of cord-rubber composite laminates, *Journal of Sound and Vibration* 197 (1996) 373–380.

[19] J.R. Banerjee, F.W. Williams, Exact dynamic stiffness matrix for composite Timoshenko beams with applications, *Journal of Sound and Vibration* 194 (1996) 573–585.
[20] S.R. Marur, T. Kant, Free vibration analysis of fiber reinforced composite beams using higher order theories and finite element modeling, *Journal of Sound and Vibration* 194 (1996) 337–351.
[21] F. Kadioglu, R. Pidaparti, Composite re-bars shape effect in reinforced structure, *Composite Structures* 67 (2005) 19–26.
[22] ANSYS (6.1), *The General Purpose Finite Element Software*, Swanson Analysis System, Inc., Houston, Texas.
[23] S.S. Rao, *Mechanical Vibrations*, third ed., Addison-Wesley, New York, 1995.